

AD-A119 927

REGIS COLL RESEARCH CENTER WESTON MA
PROJECTS IN COMPUTER AIDED CLIMATOLOGY.(U)
JUL 81 J C METTAUER

P/G 4/2

UNCLASSIFIED

AFGL-TR-81-0314

F19628-78-C-0153
NL

10-1
2
10/20/81



END
DATE
FILMED
11 82
DTIC

AD A119927

AFGL-TR-81-0314

PROJECTS IN COMPUTER AIDED CLIMATOLOGY

Jack C. Mettauer

Regis College Research Center
235 Wellesley Street
Weston, Massachusetts 02193

Final Report
1 July 1978 - 31 June 1981

July 1981

Approved for public release; distribution unlimited

FILE COPY

DTIC

Unclassified

SECURITY CLASSIFICATION OF THIS PAGE (When Data Entered)

REPORT DOCUMENTATION PAGE		READ INSTRUCTIONS BEFORE COMPLETING FORM
1. REPORT NUMBER AFGL-TR-81-0314	2. GOVT ACCESSION NO. AD-A119927	3. RECIPIENT'S CATALOG NUMBER
4. TITLE (and Subtitle) Projects in Computer Aided Climatology		5. TYPE OF REPORT & PERIOD COVERED Final 1 July 1978 - 31 June 1981
		6. PERFORMING ORG. REPORT NUMBER
7. AUTHOR(s) Jack C. Mettauer		8. CONTRACT OR GRANT NUMBER(s) AF19628-78-C-0153
9. PERFORMING ORGANIZATION NAME AND ADDRESS Regis College Research Center 235 Wellesley Street Weston, MA 02193		10. PROGRAM ELEMENT, PROJECT, TASK AREA & WORK UNIT NUMBERS 62101F 667009AA
11. CONTROLLING OFFICE NAME AND ADDRESS Air Force Geophysics Laboratory Hanscom AFB, Massachusetts 01731 Monitor/Eugene Bertoni/LYD		12. REPORT DATE July 1981
14. MONITORING AGENCY NAME & ADDRESS (if different from Controlling Office)		13. NUMBER OF PAGES: 76
		15. SECURITY CLASS. (of this report) Unclassified
15a. DECLASSIFICATION/DOWNGRADING SCHEDULE		
16. DISTRIBUTION STATEMENT (of this Report) Approved for public release; distribution unlimited.		
17. DISTRIBUTION STATEMENT (of the abstract entered in Block 20, if different from Report)		
18. SUPPLEMENTARY NOTES		
19. KEY WORDS (Continue on reverse side if necessary and identify by block number) Climatology Data Base Computergraphics Photometric Cartography Clouds		
20. ABSTRACT (Continue on reverse side if necessary and identify by block number) The detailed development of two climatological data bases are presented. The first is a photographic sky cover data base from Columbia, Missouri consisting of the Regis College Research Center's interpretations of over 2800 photographs of the whole sky. It also contains point information taken from the photographs and concurrent NWS sky cover observational information.		

DD FORM 1 JAN 73 1473

-1-

Unclassified

SECURITY CLASSIFICATION OF THIS PAGE (When Data Entered)

Unclassified

SECURITY CLASSIFICATION OF THIS PAGE(When Data Entered)

20. (continued)

An analysis of the content of the data base, the derivation of sky cover frequency density relations, a comparison of other data from ETAC-USAF observations and an interval consistency study are included in this subsection.

A second data base is taken from radar echo observations gathered from seventeen stations around the USA for a period of three years. The informational content of this data base is also summarized.

The second half of the report is a description of an interactive computer geopolitical mapping system of data displayed on the entire globe or regions of it. It is based on the Lambert azimuthal equal area projection. Development of the system, including coordinate systems, the equations of projection, and contour/map production, is discussed in detail.

The emphasis ~~of the report~~ is to explore means of bringing the power of modern computing facilities to bear on the problems of climatology. Examples are taken from projects of current climatological interest to the Air Force.

Accession For	
NTIS GRA&I	<input checked="checked" type="checkbox"/>
DTIC TAB	<input type="checkbox"/>
Unannounced	<input type="checkbox"/>
Justification	
By	
Distribution/	
Availability Codes	
Dist	Avail and/or Special

A

COPY
INSPECTED

TABLE OF CONTENTS

LIST OF TABLES	4
LIST OF FIGURES	5
INTRODUCTION	6
SECTION I: THE CONSTRUCTION OF TWO CLIMATOLOGICAL COMPUTER DATA BASES	8
SUBSECTION I-A: THE COLUMBIA MISSOURI PHOTOGRAPHIC SKY COVER DATA BASE	10
§I-A-1: The Original Data	10
§I-A-2: The Culling of Questionable Observations from the Data Base	15
§I-A-3: The Final Form of the Columbia Data Base	18
§I-A-4: A Summary of the Content of the Columbia Data Base	21
§I-A-5: A Historical Note on the Frequency Densities of Cloud Cover.	29
§I-A-6: The Seventeen Points.	34
SUBSECTION I-B: THE RADAR ECHO DATA BASE	40
§I-B-1: The Radar Echo Data	40
§I-B-2: Culling the Radar Echo Data	43
§I-B-3: The Final Form of the Radar Echo Data Base	46
SECTION II: A GEOGRAPHIC COMPUTER DISPLAY SYSTEM	51
SECTION PREFACE	54
SUBSECTION II-A: THE EQUATIONS OF TRANSFORMATION	54
SUBSECTION II-B: TWO TYPES OF REGIONS.	59
SUBSECTION II-C: DRAWING ARCS OF LATITUDE AND LONGITUDE CIRCLES: THE INTERSECTION PROBLEM.	63
SUBSECTION II-D: CONTOURS AND GEOPOLITICAL BOUNDARIES	67
SUBSECTION II-E: THE CUEING SYSTEM: INTERACTIVE USE OF THE SOFTWARE.	72
SUBSECTION II-F: THE STATE OF COMPLETION	74
BIBLIOGRAPHY	76

LIST OF TABLES

I-A-6	Enumeration of Observations by Month and Year	25
I-A-7	Enumeration of Observations by Month and Number of Tenths of Cloudiness Measured by Regional Photographic Interpretation (RPI)	26
I-A-8	Enumeration of Observations by Month and Tenths of Cloudiness Taken from NWS Observations	27
I-A-9	Selected Details of the Photographic Interpretation Density and Distribution	28
I-A-10	Comparison with Percent Relative Frequency Densities from Several Other Stations	32
I-A-11	Points versus Subregions.	38
I-A-12	Comparison of Point Ratios to Surrounding Subregion(s) Ranked in Eighths	39
I-B-1	The List of Stations Reporting Radar Echo Data Used in This Study	47
I-B-2	Card Format of Radar Echo Data	48
I-B-3	The Two Digit Hexidecimal Classification System	49
I-B-4	Itemization of Data Contained in Radar Echo Base	50
II-A-1	Contraction of Infinitesimal Area Elements	58

LIST OF FIGURES

I-A-1	A Whole Sky Photograph	9
I-A-2	Card Formats	13
I-A-3	The Face of the Projection Screen.	14
I-A-4	UPDATE output Sample	20
I-A-5	The Ranking System in Tenths	24
II-A-1	Photograph of Globe and Projection	52
II-A-2	Coordinate Systems of the Projection	53
II-B-1	Map of One Hundred and Twenty Degree Cameo Type Region . .	61
II-B-2	Several Other Cameo Type Regions	62
II-E-1	Example of Interactive Query System	71

INTRODUCTION

Projects in Computer Aided Climatology is a report on the work performed by Regis College Research Center under Air Force contract AF-19628-78-C-0153 during the period between July 1, 1978 and June 30, 1981. It is not inclusive of all efforts made by the Center under this contract. Several projects are reported on in considerable detail. They are examples of the type of activities that were perceived as being the most productive research activities that could be performed in fulfillment of the stated objectives of the contract.

These activities are: 1) the construction of climatological computer data bases facilitating the formulation and testing of mathematical/statistical hypothesis and models and 2) the development of computer aided technology for summarizing and communicating results derived either directly from empirical data or from theoretical activities of analysis and interpretation of scientific inquiry, not a substitute for them. They bring the vast power of the electronic information processing revolution creatively to the aid of the atmospheric scientist and mathematician.

The report is divided into two sections. Section one gives the details of the construction of two climatological data bases. The process and criteria for culling raw data, the ordering and merging of data, and the format of the final form of the bases is described. The informational contents of both bases are summarized. Several applications of one of the data bases and a comparison to other related collections of data are presented.

Section two is a description of a computer geopolitical mapping system intended for presenting climatological and meteorological information. The system is interactive and makes use of the Lambert azimuthal equal area projection which was suggested to Regis by Irving Gringorten of AFGL. This project in computergraphics, although more difficult than initially anticipated, was surprisingly satisfying for the author and the student assistants to work on.

This report is to act as a guide to subsequent workers on similar projects. This is especially true of Section II. The totality of work outlined has been tested for feasibility but not all of it has been added to the existing system as a final piece of software. An attempt is made to indicate what is needed in the future and how to do it.

The author would like to express his gratitude to those members of the Regis community who assisted in this effort, especially to the student employees of the Research Center, to Marion Polzella, J.D., the present director of the Research Center and to Sister Mary Anne Doyle, Ph.D., her predecessor. Very special recognition must be paid to Sister Leonarda Burke who inspired all of us at the Research Center through her life long dedication to diligent mathematical and scientific research.

Also Sister Ann Marie Grady, C.S.J. is responsible for preparing the photograph of Figure II-A-1 on page 52. Miss May Ngan of the Research Center should be recommended for canonization for her efforts and patience on typewriting the first draft of this manuscript.

SECTION I

THE CONSTRUCTION OF TWO CLIMATOLOGICAL COMPUTER DATA BASES



FIGURE I-A-1

A Whole Sky Photograph

The above is a representative whole sky photograph which is included in the following study. The National Weather Service judged the sky to be 70% cloudy in a concurrent observation. The Regis regional photograph interpretation is shown in Figure I-A-4. The sun disk and the anemometer stand are seen in the photograph. This photograph was taken at 1500 LST on June 10, 1966.

These photographs were originally taken to aid in estimating the probability of cloud-free-lines-of-sight which were required for determining the utility of optical and infrared search and tracking systems. Earlier attempts to determine such probabilities including sunshine meters and satellite photographs had been found to be inaccurate [1].

SUBSECTION I A

THE COLUMBIA, MISSOURI PHOTOGRAPHIC SKY COVER DATA BASE

1. The Original Data

The original data consisted of slightly less than 3000 whole sky photographs collected at Columbia, Missouri and a concurrent collection of National Weather Service (NWS) observations. The photographs were taken at 0900, 1200, and 1500 LST between March 1966 and September 1969. There were several durations of time during this period when photographs were not taken because of equipment malfunction (c.f., Subsection I-A-3 of this report for the effect that this had upon the seasonal composition of the data).

Reference [1] gives a complete description of the photographic techniques and equipment employed, it also gives an elaborate description of the larger collection of photographs taken at Columbia. For completeness, a few details will be given here. The photos were taken using a Nikon camera, a specially ground fish-eye lens, a lens cover, and a sun shield which followed the disk of the sun (used to prevent over exposure of the film). The film/filter combination was most sensitive to infrared which produces greater contrast between cloud and blue sky than would be observed by the naked eye. This tends to slightly increase the amount of cloudiness observed. The paper of Lund, Grantham and Davis [2] presents a comprehensive description of the data selected for this data base. Figure I-A-1 is a representative sample of a whole sky photograph analyzed under this Regis contract.

The NWS data were sent to Air Force Cambridge Research Laboratories on 80-column Hollerith cards. The format of these cards is given in Figure I-A-2. Out of over three thousand cards, only three were found to be defective by the criteria of improper characters in fields. A very small number of the reporting times were missing from the data sent.

The selected photographs were interpreted and also transcribed to Hollerith cards in 1977 by the Regis College Research Center, using the following techniques.

The photographs, which are contained in reels of 35-mm transparencies, were projected by means of a film transport and projected onto the screen which was stationed in a darkroom. The image was adjusted and focussed so that the outer rim of the photograph aligned with the outer circle on the screen. The orientation of the photograph could be checked by observing the position of an anemometer stand and water tower (see the example of a whole sky photograph given in Figure I-A-1).

The circular region of each photograph, corresponding to *elevation* angles greater than five degrees, was subdivided into one hundred and eighty five subregions of approximately equal area. The outer rim, corresponding to elevation angles of less than five degrees, was ignored because of haziness and other problems complicating interpretation [2]. A drawing of the entire circular region of the photograph, the concentric inner circular region of *elevation* angles greater than five degrees, and the boundaries of 185 subdivisions were drawn on the face of a projection screen. In addition, seventeen small circles (each of area less than 1% of the area of any of the subregions) were also drawn on the screen.

Figure I-A-3 portrays the configuration on the face of the projection screen.

For each photograph, the cloudiness of each of the 185 subdivisions, was ranked in eighths and an integer between 0 and 8 was recorded in a corresponding column on the coding sheets. Also each of the seventeen small circles were ranked either "0" or "1". A "1" was assigned if and only if the center of the circle was contained in cloud of any sort or size. This information was also recorded on the coding sheets and later punched on 80 column Hollerith cards at the Research Center. This information required three cards for each photograph and thus the complete data for each observation time were contained on four cards. The first card in order was the NWS data card and the next three cards were photo data cards prepared by Regis. The complete format of all cards is shown in Figure I-A-2. Observations were included in the study initially, if and only if, both the photograph and the NWS card existed.

a) NWS DATA CARD FORMAT	b) PHOTO DATA CARD 1	c) PHOTO DATA CARD 2	d) PHOTO DATA CARD 3
<u>COL</u> <u>USE</u> 1-2 YEAR (66, 57, 58, 69) 3-4 MONTH (1-13) 5-6 DAY (1-31) 7-8 HOUR (09, 12, 15) 9 ALWAYS BLANK 10-12 SKY AND CEILING 14-15 OBSTRUCTION TO VISION 25-26 TOTAL SKY COVER 28-34 FIRST LAYER (AMT, TYPE, HGT) 36-42 SECOND LAYER (AMT, TYPE, HGT) 45-46 SUMMATION TOTAL 48-54 THIRD LAYER (AMT, TYPE, HGT) 56-57 SUMMATION TOTAL 59-63 FOURTH LAYER (AMT, TYPE, HGT) 55-66 OPAQUE SKY COVER	<u>COL</u> <u>USE</u> 1-2 SAME AS a) 3-4 SAME AS a) 5-6 SAME AS a) 7-8 SAME AS a) 9 1 10-66 SUBREGION RANKS IN EIGHTHS (1-57) 71-80 POINTS A-I	<u>COL</u> <u>USE</u> 1-2 SAME AS a) 3-4 SAME AS a) 5-6 SAME AS a) 7-8 SAME AS a) 9 2 10-73 SUBREGION RANKS IN EIGHTHS (58-121) 77-90 POINTS J-M	<u>COL</u> <u>USE</u> 1-2 SAME AS a) 3-4 SAME AS a) 5-6 SAME AS a) 7-8 SAME AS a) 9 3 10-73 SUBREGION RANKS IN EIGHTHS (122-185) 77-80 POINT N-Q

FIGURE I-A-2

Card Formats

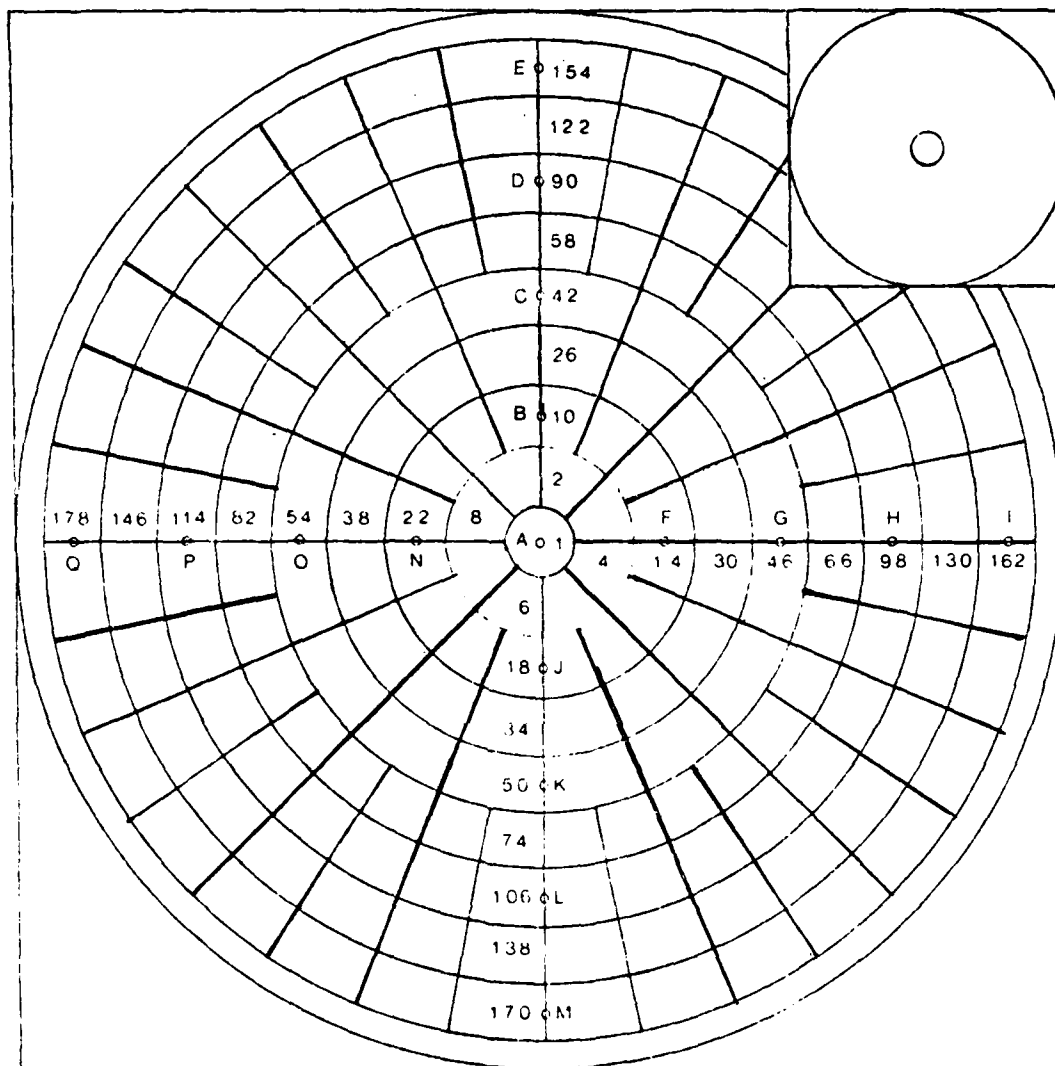


FIGURE I-A-3

The Face of the Projection Screen

The above drawing is a reduction of the geometric figure drawn on the projection screen. The actual *radius* of the outer circle on the screen was 29 cm. compared to 7.7 cm. in the above drawing. The seventeen points are located in the center of the small circles. For the sake of legibility neither the circles nor the alphanumeric characters are drawn to scale. The upper right hand cut away is the actual size of the innermost circle (Zenith angle 5°). The small circle for point A is also drawn to scale in the cut away.

2. The Culling of Questionable Observations from the Data Base

After the cards were ordered and merged by computer, the entire file was made into an UPDATE "program library". UPDATE is a CDC utility whose function is to facilitate insertion, deletion and modification of card images to a computer file which is called a "program library" (PL). In addition, UPDATE also automatically keeps a chronological history of all changes made to the PL. This record is kept as part of the PL itself and is passed from one generation to the next. UPDATE permits the user the option of purging any portion of the PL history. Using the appropriate directives, a user may restore unpurged inactive data to active status in the program library. Figure I-A-4 is a copy of part of one page of the current UPDATE listing of the data base.

The photo data punched at Regis was carefully checked by the CDC 6600 for 1) improper characters in each data field, 2) improper values in any field, and 3) impossible times or dates. A listing of all suspected data was compiled and checked against the coding sheets for correction. New cards were punched and automatically inserted using UPDATE. The resulting data set consisted of 2931 observations or 11,724 card images which were saved on nine track magnetic tape, system disk permanent files and a private disk pack.

For each observation Q the sum of the number of eighths of cloudiness in all of the one hundred and eighty-five subregions was computed. This quantity will be denoted as $\Sigma(Q)$ and $0 \leq \Sigma(Q) \leq 1480$. The number $\Sigma(Q)/148.0$ will be called $\sigma^*(Q)$ or the raw sigma rank of observation of

Q and the rank of observation Q in tenths will be denoted as $\sigma(Q) = [\sigma^*(Q) + .5]$.¹ The raw rank σ^* is a continuous variable between 0 and 10 while σ is one of the eleven integers 0 to 10.

A comparison of the σ ranks for each observation with the v rank (the number of tenths of cloudiness reported by NWS) was made by computer and a list of those observations for which the raw $\sigma^*(Q)$ score differed from $v(Q)$ by more than two was prepared. The coding sheets were checked for each of these observations. If any error was found, new cards were punched and inserted. If the cards were an accurate copy of the coding sheet data and the discrepancy was serious, the photographs themselves were reexamined. In some cases, the photographs were found to be defective, i.e., over, under or multiply exposed or, in a few cases, the lens cover was apparently dirty or obscured by condensation. In such cases, the data was removed from the study.

In a few other cases, the photographs seemed to have no relation to the NWS observation. These observations were also eliminated from the data base under the assumption that they were out of chronological order. Other photographs checked at the same time seemed to correspond well with NWS information but the interpretation of photographs contained on the coding sheets seemed questionable. It was felt that simply reinterpreting those that did not agree with NWS observations and leaving those that did, would introduce an unacceptable chance of bias in the resulting statistics. If any photograph in a NWS category (those observations with the same value

¹Bracket Notation: $[x]$ designates largest integer less than x if $x > 0$.

of v) was to be reinterpreted, then the entire NWS category was to be reinterpreted. This led to the reinterpreting and repunching of all data from $v = 4$ to $v = 9$. This encompassed nearly 25% of all observations.

The reinterpreted data contained no "large" (> 2.0) differences between photo observations and NWS observations and the agreement seemed superior to the first interpretations. In a few cases, (the photo shown in Figure I-A-1 for instance) repeated reinterpretation did not improve the argument between photograph and NWS data, however, the argument was marginally within the tolerance of $|\sigma(Q) - v(Q)| \leq 1$ accepted in this study. Both methods of estimating total sky cover, of course, involve human judgments. When the sky is broken into many small disconnected regions of cloudiness, such as is the situation in Figure I-A-1, judgment by either method seems to be strained and what is seen on the photograph is influenced by the film and the camera lens. The final RMS difference, for the entire sample, between the raw σ^* and v scores for each observation was .7. Of the original observations, 2808 remained. The point data was not used to determine if an observation was to be kept.

3. The Final Forms of the Columbia Data Base

The data base now has two forms: one is the UPDATE program library which has previously been described and the second is a shortened form which is more convenient and is less expensive to work with for statistical analysis but does not contain any NWS information other than the value of v for each observation.

The program library form of the data base was edited in late 1978. The new library generated consisted of all old card images with the reinterpreted ones replacing their predecessors. The chronological record of changes contained in the library started fresh at this time. The chronological record of previous changes were destroyed. The immediate predecessor of each reinterpreted observation was saved with inactive status in the new PL. Figure I-A-4 is a sample of a small portion of the PL listing. Active cards are marked with an "A" on the right hand side; inactive with an "I". The old data can be restored individually or en-mass by the use of the proper directives to UPDATE. This UPDATE program library is saved on private disk pack STDATA as permanent file CLOUD. It is also saved on 9-track magnetic tape SKY001. It is important for any user to remember that UPDATE files cannot be copied by any other CDC utility and must be processed by UPDATE itself.

The second form of the data base requires only 14 records per observation as opposed to 32 for the longer version. Each record consists of data from one hundred observations (or 1400 words). The file is in "long stranger" type records and is suitable for FORTRAN BUFFER IN statements which were chosen because of economical

factors. This form of the data base is intended for operational use and is regenerated from the UPDATE program library before periods of applications. It requires less than 45 seconds to generate from the program library and it has not seemed worth-while to save it between periods of use.

It was mentioned in Subsection I-A-1 that the equipment malfunctioned during certain periods. Also, nearly two-hundred observations were eliminated as described in Subsection I-A-2. Thus, it was not expected that the seasonal distribution of observations would be uniform. Of the final 2808 observations, 24.5% were taken in the spring, 30.1% in the summer, 21.5% in the autumn and 23.9% in the winter (see Table I-A-6).

4. A Summary of the Content of the Columbia Data Base

References [1], [2], and [3] in the bibliography are concerned with the Columbia whole sky photographs. Paper [2] uses the Regis data base for all of its studies, however, only 2805 of the 2808 observations were utilized since three photographs of the 2808 still remaining in the data base have been determined to be of questionable quality. Paper [3] provides an example of the application of information contained in the data base pertaining to the spatial distribution of cloudiness.

Table I-A-6 is a summary of the monthly distribution of cloudiness. Table I-A-7 and I-A-8 reveal the remarkable characteristics of the frequency density of cloudiness: the extreme categories zero and ten (0-5% and 95-100% cloudy) comprises over one half of the total number of observations and only ten percent of the range of cloudiness. This is true for both regional photographic interpretation (RPI) and the NWS observations. The extremeness is slightly more pronounced for the RPI than NWS observations.

Table I-A-9 emphasizes the extremal nature of the data. The extremal cases here are represented by ranks 0 and 1480. The first of these is the category of photographs for which less than one eighth of cloudiness is reported for each subregion. The second is the category for which every subregion is reported to be totally overcast. These two categories, together comprising only one fourteen hundred and eightieth¹ of the total

¹The two extreme ranks "0" and "1480" each are "half ranks" (i.e., each represent on 1/2 the length of the other 1479 equal length intervals.) See Figure I-A-6.

range of cloudiness (each subregion is presumed to be ranked 0 only if one sixteenth or less is cloudy). contain forty-two percent of the total number of observations.

Table I-A-10 presents the frequency density functions for the total period of observations taken at several different locations in the United States. The data was extracted from a few of the ETAC-USAF observation stations mentioned above. Relative frequency densities from the Regis data base (RPI, NWS and point photographic interpretation (PPI) to be discussed later) are presented in the same table for ease of comparison. In addition, relative frequencies from the Columbia, Missouri ETAC-USAF data specific to the hours 0900-1400 LST are included. These numbers are averaged to account for the monthly variations of quantity of observation in both samples.¹

Examination of ETAC-USAF cloudiness data reveals that at nearly every station in the United States for which data was available, the extremal categories (rank 0 and rank 10) account for forty or more percent of the total observations tallied over the entire period of observation for that station. The occurrence of any hour, at any month, from any given station in which an internal category contains more observations than the sum of the two extremal categories, is rare. Exceptions are most frequent during summer months, at midday, at locations with warm moist climates. A study, Reference [4], of size, altitude, number and cover distributions of cumuli

¹ Since the ETAC-USAF data is presented in two hour groupings (0900-1100, 1200-1400 and 1500-1600 LST) either the last grouping had to be ignored or weighed in with an arbitrary coefficient. The former option was taken.

near Pensacola, Florida, using daytime August data, supports a conjecture that extremalness is minimal when the cover is predominately of small scale size (presumably cumulus) clouds.

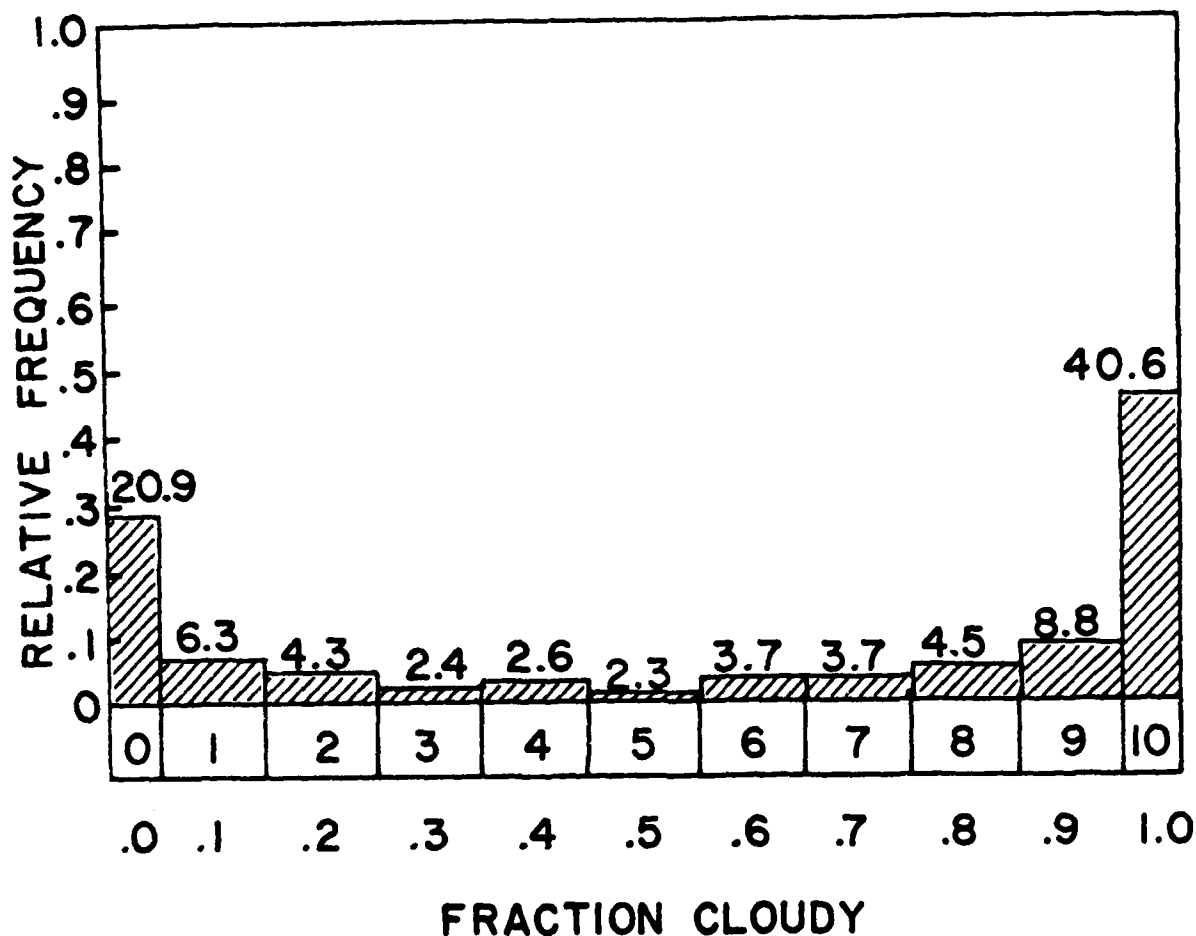


FIGURE I-A-5

The Ranking System in Tenths

The above histogram of relative frequency versus fraction of sky cloudy for regional photographic interpretation of the Columbia data is presented to illustrate the ranking system in tenths used in this report.

Rank $k = 0$ is the collection of all data with less than five percent of the sky cloudy.

Rank $k = 10$ is the collection of data with more than ninety-five percent of sky cloudy.

For other values of k , i.e., $k = 3$, rank consists of all data with twenty-five percent of the sky cloudy and less than or equal to thirty-five percent cloudy.

The ranks $k = 0$ and $k = 10$ comprise, in this case, one tenth of the range of cloudiness but contain sixty-one and one half percent of all data.

The same idea is used for the eighths and 1/1480 ranking systems. The combined range of the two extremal ranks equal the range of ordinary rank.

	1966	1967	1968	1969	TOTAL
JAN	0	84	81	59	224
FEB	0	78	72	61	211
MAR	62	73	90	0	225
APR	71	78	81	0	230
MAY	65	82	86	0	233
JUN	67	73	70	39	249
JUL	71	91	85	74	321
AUG	77	75	79	44	275
SEP	58	84	50	0	192
OCT	75	64	71	0	210
NOV	71	54	77	0	202
DEC	73	84	79	0	236
TOTAL	690	920	921	277	2808

TABLE I-A-6
Enumeration of Observations by Month and Year

	JAN	FEB	MAR	APR	MAY	JUN	JUL	AUG	SEP	OCT	NOV	DEC	TOTAL
0	39	46	49	43	59	31	62	46	45	72	46	48	586
1	7	13	8	19	10	21	29	22	8	14	13	12	176
2	7	11	6	4	9	16	21	19	8	9	3	7	120
3	6	3	3	4	3	12	13	9	4	8	2	1	68
4	1	4	6	7	5	8	10	13	6	12	0	1	73
5	3	2	3	4	6	5	12	14	4	4	4	5	66
6	5	7	3	5	8	12	23	14	7	7	6	6	103
7	7	4	7	8	7	9	20	16	6	6	7	6	103
8	3	9	9	10	13	17	24	18	6	4	6	7	126
9	16	8	24	23	16	33	36	22	23	14	16	16	247
10	130	104	107	103	97	85	71	82	75	60	99	127	1140
TOTAL	224	211	225	230	233	249	321	275	192	210	202	236	2808

TABLE I-A-7

Enumeration of Observations by Month and Number of
Tenths of Cloudiness Measured by Regional Photographic Interpretation (RPI)

The right most column is the frequency density in tenths
for the entire data base.

	JAN	FEB	MAR	APR	MAY	JUN	JUL	AUG	SEP	OCT	NOV	DEC	TOTAL
0	35	42	45	35	47	30	52	40	43	68	43	40	520
1	7	13	7	8	14	14	17	15	3	11	11	7	127
2	7	6	6	16	7	13	23	15	11	11	3	13	131
3	4	10	8	8	12	14	22	14	12	16	5	9	134
4	8	5	5	5	5	13	20	23	1	10	4	3	102
5	5	6	3	7	5	8	14	15	5	4	2	4	78
6	4	7	5	7	10	11	24	19	6	8	5	7	113
7	6	5	7	9	9	12	27	15	10	5	5	4	114
8	8	8	11	11	13	25	26	21	5	8	9	7	152
9	12	11	14	18	9	23	24	15	14	9	17	12	178
10	128	98	114	106	102	86	72	83	82	60	98	130	1159
TOTAL	224	211	225	230	233	249	321	275	192	210	202	236	2808

TABLE I-A-8

Enumeration of Observations
by Month and Tenths of Cloudiness Taken from NWS Observations

	0	1	2	3	4	5	6	7	8	9
0	416 .296 .148	3 .001 .149	3 .001 .150	3 .001 .151	3 .001 .152	6 .002 .154	4 .001 .155	5 .002 .157	5 .002 .159	4 .001 .160
10	5 .002 .162	2 .001 .163	2 .001 .164	3 .001 .165	3 .001 .166	2 .001 .167	5 .002 .169	5 .002 .171	2 .001 .172	5 .002 .174
20	5 .002 .176	1 .000 .176	1 .000 .176	0 .000 .176	4 .001 .177	2 .001 .178	3 .001 .179	1 .000 .179	4 .001 .180	1 .000 .180

1450	7 .002 .383	7 .002 .385	7 .002 .387	5 .002 .389	2 .001 .391	7 .002 .392	10 .004 .394	12 .004 .398	12 .004 .402	6 .002 .406
1460	7 .002 .408	4 .001 .410	5 .002 .411	6 .002 .413	11 .004 .415	4 .001 .419	6 .002 .420	5 .002 .422	9 .003 .424	9 .003 .427
1470	2 .001 .430	11 .004 .431	9 .003 .435	10 .004 .438	9 .003 .442	9 .003 .445	7 .002 .448	2 .001 .450	1 .000 .451	1 .000 .451
1480	771 .549 1.000									

TABLE I-A-9

Selected Details
of the Photographic Interpretation Density and Distribution

The data in the table is listed for some of the 1481 ranks of the photographic data. The top integer N_r for rank [$r = \text{ROW plus COLUMN}$] is the number of photographs with r fourteen hundred and eightieths of cloudiness for the entire photograph. The middle number is the value of the empirical probability density function: $P_r = (N_r/N_s)(\Delta x/\Delta x_r)$ where N_s is the sample size (2808), $\Delta x = 1/1480$ and $\Delta x_r = \Delta x/2$ for $r = 0$ and $r = 1$ and Δx otherwise. The bottom number is the empirical probability distribution function P_r :

$$P_r = \sum_{k=0}^r P_k \Delta x_k.$$

5. A Historical Note on the Frequency Densities of Cloud Cover

The property referred to as extremalness in § I-A-4 was noted by Karl Pearson in 1898 [5]. Pearson had theoretically anticipated the existence of natural phenomenon with what he referred to as a "U-shaped distribution", in an earlier memoir on skew variance. At the time of this prognostication, Pearson had no satisfactory example of such data. The occasion of the publication [5] was to report that a Hugo Meyer of Berlin had published a study of the "degrees" of cloudiness measured at Breslau. The study consisted of 3653 daily observations made during the decade 1876-1886 of cloudiness ranked in tenths. This data is reproduced as percentage relative frequencies in Table I-A-10 of this report. In [5], Pearson examines the moments and other parameters of this first example of "U-shaped distributions".

Pearson remarks, "... the method used for determining the extent of cloudiness is not entirely satisfactory, and, as Herr Meyer remarks, the observer must have had some personal bias with regard to the grade 9 ..." on Page 287 [5]. This is a comment on the reduced probability between rank 8 and rank 10 (5.0 to 3.0 to 57.1) seen in the Breslau data in Table I-A-10. The opinion of Pearson and Meyer, considering the amount of data that they had access to, was certainly not unreasonable. Today, when hundreds of thousands of observations have been gathered from scores of locations, and it is known that densities often show similar depressions at rank 1 and also very frequently at rank 9, it is still believed by many climatologists that observational bias accounts for the local minima adjacent to the extreme ranks.

Considering that: a) ETAC-USAF observations show that these blips occur at most locations when tallied over the complete period of the study, but seldom happen at every hour and at every month for any given location, and b) that there appears to be predictability to the times of maximum and minimum depressions; a fundamental relationship to other climatological factors should not be dismissed. As with extremeness of the density, these depressions on casual examination seem to relate to scale size of the clouds (cumulus in day, cirrus during night hours).

Studies utilizing existing data, and selected experiments using modern photometric technique could be used to choose between the hypotheses of observational bias and of functional relationship to other climatological factors. Computer interpretation of the photographic images would minimize the human bias factor and would, in this way, be superior to the Regis method of interpretation, which still contains the possibility of human bias in the interpretation of the subregion ranks in eighths. The current study is equivocal on this point. The adjusted ETAC-USAF data shows no local minima at rank 1 or 9 and neither does the RPI data. The concurrent NWS data shows a slight dip at rank 1 (18.4 to 4.5 to 4.7). Several slight depressions appear in the monthly RPI data (Table I-A-8).

Accurate, complete and insightful knowledge of the frequency density of cloudiness is indispensable to a meaningful study of the temporal variation of percent cloudiness. The density is an indirect statistical measure of the persistence of a given amount of cloudiness and thus is related to the time rate of change of the amount of cloudiness; i.e., the higher the density of cloudiness, the smaller the mean absolute time rate

of change of cloudiness. Feller devotes Chapter III of his monumental text, [6], to the "arc sine law", which is a model of a special case of an extremal density related to the one step random walk problem associated with the experimental flipping of a "fair" coin.

Specifically, the "arc sine law" defines the density of "first passage times" for this problem. The name "arc sine law" derives from approximating the integral of $f(s) = 1/(\pi\sqrt{s-s^2})$ over the interval $[0,x]$ by the expression $(2 \arcsin \sqrt{x}) / \pi$. More general, one step random walk problems are related to other extremal functions in subsequent chapters of [6]. No simple relationship has yet been determined between cloudiness and one step random walk processes. Eventually, this may provide a clue to modeling the stochastic relationship between cloudiness and temporal-spatial parameters.

TABLE 1-A-10

LOCATION	% EXTREME	0	1	2	3	4	5	6	7	8	9	10
AGENCY YRS SAMPLE												
ADAK AK	62.7											
NS 46-65 166936	1.0	0.6	1.3	2.1	2.5	2.4	2.9	5.9	10.1	8.6	61.7	
AMARILLO TX	62.7											
WBAS 46-68 171069	39.2	5.2	4.7	4.4	3.6	2.7	3.5	4.1	5.0	4.2	23.5	
BILLINGS MT	62.0											
48-70 165203	21.0	5.0	5.8	4.9	4.5	2.4	5.6	5.6	7.6	6.7	31.0	
BOSTON MA	65.5											
WBAS 45-65 176710	24.9	4.2	4.5	4.0	3.3	2.3	2.8	3.6	5.0	4.8	40.6	
CHEYENNE WY	53.7											
WBAS 48-67 155850	27.9	6.1	5.1	4.7	3.5	3.3	4.5	5.1	6.3	7.8	25.8	
COLUMBIA MO	66.8											
NWS 46-73 192548	31.4	4.2	4.3	4.2	3.4	1.9	3.1	3.7	4.6	4.1	35.4	
FORT HUACHUCA AZ	58.6											
AEPG 54-69 125350	42.7	5.9	4.9	4.7	4.1	3.5	3.9	4.5	5.3	4.6	15.9	
FRESNO CA	75.2											
WBAS 49-68 145503	54.4	3.6	3.1	2.9	2.1	1.6	2.1	2.8	3.2	3.5	20.8	
JACKSONVILLE FL	43.4											
NAS 45-68 203051	20.4	4.2	5.8	6.0	5.6	5.4	5.3	7.3	9.6	7.4	23.0	
KEY WEST FL	24.8											
NAS 53-68 135147	11.9	7.3	9.1	10.8	9.1	9.3	5.8	8.2	9.8	5.8	12.9	
WICHITA KS	61.3											
AFB 48-67 169269	31.5	5.7	4.8	4.4	3.6	3.0	3.2	3.9	5.3	4.8	29.8	

TABLE I-A-10 (Continued)

LOCATION AGENCY	% EXTREMAL YRS SAMPLE	0	1	2	3	4	5	6	7	8	9	10
BRESLAU POLAND 1876-1885	77.7 3653	20.6	4.9	2.9	1.8	1.2	.3	.5	1.9	5.0	3.0	57.1
COLUMBIA MO REGIS 66-69	61.5 2808	20.9	6.3	4.3	2.4	2.6	2.3	3.7	3.7	4.5	8.8	40.6
COLUMBIA MO REGIS 66-69	64.1 2808	20.5	5.1	4.3	1.6	3.0	3.9	3.6	1.8	5.2	7.2	43.6
COLUMBIA MO REGIS 66-69	59.8 2808	18.5	4.5	4.7	4.8	3.6	2.8	4.0	4.1	5.4	6.3	41.3
COLUMBIA MO NWS 64-73	58.8 48141	21.7	4.7	4.1	4.5	3.9	2.7	3.9	4.6	6.0	6.3	37.1

REGIONAL PHOTOGRAPHIC INTERPRETATION
POINT PHOTOGRAPHIC INTERPRETATION
CONCURRENT NWS DATA
ADJUSTED DATA FROM 0900-1400 LST

TABLE I-A-10

Comparison with Percent Relative Frequency Densities from Several Other Stations

The first eleven entries are taken from ETAC-USAF data. The last entry is the ETAC-USAF data for Columbia for the years 1964 - 1973 using the adjustments described in subsection I-A-4.

The Breslau data is from the study discussed in subsection I-A-5 as reported by Karl Pearson.

6. The Seventeen Points

A simple indicator of cloudiness was devised using the seventeen binary values $V_a(Q)$ (the value corresponding to points $a \in \{a,b,c,\dots,q\}$ for observation Q). The formula for the indicator is:

$$\rho(Q) = 10 \left[\left(\sum_a V_a(Q) / 17 \right) + .5 \right]$$

where the bracket notation is used to indicate truncation to the largest integer less than the quantity enclosed in brackets (c.f., $\sigma(Q)$ in § Subsection I-A-2).

The range of values of $\rho(Q)$ is the set of eleven integers $\{0,1,\dots,10\}$ as is the range of $v(Q)$ and $\sigma(Q)$. The root mean square of the difference $(\sigma(Q) - \rho(Q))$ and $(v(Q) - \rho(Q))$ were computed. Their values were found to be respectively .950 and 1.15 compared with the root mean square difference of $(\sigma(Q) - v(Q))$ which was found to be .7 (c.f., § Subsection I-A-2).

The significance of these RMS differences cannot be judged by the usual means (i.e., the formula on pages 236-237 of Cramer, .7] , since the sample cannot be assumed to be normally distributed. A simple ad hoc model, not presented here, shows that for a sample with the extremal distribution of v that, if the V_k were randomly chosen for each observation, the expected value of the RMS difference $(v(Q) - \rho(Q))$ would be 4.5. The values obtained, .95 and 1.14 would, according to this model, be equivalent to the expected value of the RMS of an experiment in which the V_k were chosen randomly and, if $|v - \rho| > 3$ using the formula for ρ , the value of ρ would be readjusted so that $|v - \rho| = 0$.

Examination of the actual data reveals that the differences $|p(Q)-v(Q)|$ are occasionally quite large (e.g., five, and in one case ten) and thus on the average they must be less than one. The penalty extracted for one value of the difference being equal to ten is that one hundred must be equal to zero for the average to balance to be one over that set of one hundred and one observations. This good showing of the RMS differences is partially accounted for by the fact that the differences are usually zero for extremal observations which are in the majority.

Tables I-A-11 and I-A-12 show the agreement of the point data with the subregional data. Several of the employees involved in the photographic interpretations were questioned about point evaluation by the author. Two of them had the impression that points were the little circles and would assign a '1' if any part of the small region intersected a cloud. The third employee understood the instructions, but complained that it was difficult to determine where the center of the circle was and further felt that if she had reinterpreted some of the photographs several times, that she would have had several different results because the processes were so sensitive to the alignment of the photograph on the projection screen. The ratio $R_{\alpha k}$ are invariably higher than expected as is seen in the Table I-A-12 from the average results of the combined ratio column. This adds creditability to the possibility that the points were interpreted as small disks (i.e., as "fields-of-vision" rather than as points in the center of the disk or "lines-of-sight".) The difference between the two concepts becomes more pronounced as the scale size of the cloudy regions decreases (for an interesting elaboration of this type of phenomena, see Mandelbrot [8]).

It is on the whole satisfying that the overall results are as good as Tables I-A-11 and I-A-12 indicate considering the crude techniques employed.

Study of the point data uncovered what at first appeared to be a curious accident. Each of the binary values $V_\alpha(Q)$ are surprisingly good indicators of the status of the entire sky. The statement: if $V_\alpha(Q)$ is "0" implies that $v(Q) < .5$ and if $V_\alpha(Q)$ is "1" implies that $v(Q) > .5$, is correct over ninety percent of the time for the entire data base. The statement is equally as good for the indicators σ and ρ and is nearly independent of which point α is chosen. The best results are obtained from winter data (nearly 95%) and the poorest in summer (87%). Point A, in the center of the photograph produced consistently the best result in every season. The poorest overall performance was given by points at zenith angles of 80° , but 40° was only slightly better. Points at 20° and 60° were nearly as good as point A overall. The poorest performance was at point I in the summer. It was correct only 83% of the time.

For any point α , P_α is defined to be the probability that the indicator value $V_\alpha(Q)$ correctly represents the indicator value $v(Q)$ in the sense of the previous paragraph. The value of P_α is given by the following :

$$P_\alpha = \sum_{k=0}^4 (1-x_k) P_{k,\alpha} + \sum_{k=5}^{10} x_k P_{k,\alpha}$$

where the $\{x_k\}$ are taken to be representative values of the category rank k and the $P_{k,\alpha}$ are the relative frequencies associated with the indicator v at rank k . The representative values for numerical calculations were taken to be $\{.025, .1, .2, \dots, .9, .975\}$ respectively. (C.F. Figure

I-A-5).

Using for the $P_{k,\alpha}$ the frequency density for the indicator v (see Table I-A-10), the values of P_α for all data is .91 and for winter and summer respectively are .96 and .88 which are good approximations to the results which were empirically determined. A Simpson rule integration of the theoretical arc sine law of [4], chapt. III. (C.F. I-A-5) estimated P_α as .84 and the same technique applied to a binomial distribution with $p = 1/2$ estimated P_α for that distribution to be .67. The values of P_α increases as the extremalness of the distribution increases. Its minimum value is .5 when all density is concentrated at $x = .5$ and its maximum value is 1.0 when all density is concentrated at the two points $x = 0$ and $x = 1$.

This simple observation has potential scientific, military and commercial applications.

A	C	I	T	P	O	I	T	F	O	I	T
0	937	5	942	0	960	5	985	0	917	12	929
1	60	16	76	1	45	13	58	1	55	24	79
2	32	12	44	2	34	22	56	2	32	13	45
3	15	13	28	3	30	21	51	3	31	20	51
4	9	21	30	4	21	22	43	4	14	11	45
5	9	25	34	5	12	43	55	5	8	50	58
6	5	43	48	6	10	61	71	6	14	63	77
7	4	132	136	7	6	163	169	7	8	157	165
8	8	1462	1470	8	2	1318	1320	8	6	1353	1359
T	1079	1429	2808	T	1140	1668	2808	T	1085	1723	2808

J	O	I	T	N	O	I	T
0	904	19	923	0	969	13	982
1	65	11	76	1	52	20	72
2	26	13	39	2	23	13	36
3	17	27	44	3	18	24	42
4	15	25	40	4	17	18	35
5	6	43	49	5	9	33	42
6	5	52	57	6	14	60	74
7	16	145	161	7	12	151	163
8	3	1416	1419	8	11	1351	1362
T	1057	1751	2808	T	1125	1683	2808

TABLE I-A-11

Points versus Subregions

Data for five of the seventeen points are given above. Point A is located at the center and the other four points are on a circle of 20° radius. The ranks, in eighths, averaged over the surrounding subregion(s) of the point specified in the top left corner, are listed in the left column of each table. The total number of observations of that rank for the specified point is given in column T. The number of observations of that subregion rank are broken down into clear and cloudy respectively in columns 0 and 1.

RANK	COMBINED RATIO	POINT A RATIO	RANGE
0	.0142	.0053	0 - .0625
1	.2235	.2105	.0625 - .1875
2	.2899	.2727	.1875 - .3125
3	.4508	.4643	.3125 - .4375
4	.6458	.7000	.4375 - .5625
5	.7464	.7353	.5625 - .6875
6	.8237	.8958	.6875 - .8125
7	.9586	.9705	.8125 - .9375
8	.9941	.9946	.9375 - 1.000

TABLE I-A-12

Comparison of Point Ratios to Surrounding Subregion(s) Ranked in Eighths

Sixteen of the seventeen points are on the boundary of two subregions. Point A is the exception, being contained only in subregion 1. The expression "rank of a point" will mean the average rank in eighths of the subregions which contain, or border the point, rounded down to the nearest integer.

$R_{\alpha k}$ is the fraction of the set of all observations whose rank at point α is k , which are recorded as being cloudy (i.e., $V=1$). The combined ratio in the above table is the average of $R_{\alpha k}$ over all seventeen points.

If the ranking of subregions and points were done accurately and according to instructions, it would be expected that the combined ratios should fall the range given in the right most column. Except for rank $k=8$ the combined ratios are higher than the top of the range. The individual values of $R_{\alpha k}$ (R_{Ak} is given in Table I-A-12) also usually are above the range. This is suggestive that human observers always interpret "point" as "small region".

SUBSECTION 1-B

THE RADAR ECHO COMPUTER DATA BASE

1. The Radar Echo Data

The data for this study were gathered from seventeen different weather stations around the United States. These stations are itemized in Table I-B-1. The study persisted for a three-year period; from January 1, 1973 until December 31, 1975. Information was to be reported regularly at three-hour intervals, and the time was to be reported in LST for each station. It was understood from the beginning that there would have to be allowance for some missing observations. This is discussed later in this subsection.

The following instructions were given to each station:

- a) Every three hours a photograph was taken of the radar scope with the antenna elevation angle at 0° .
- b) If the 0° elevation angle was clear, the data for the observation consisted only of the 0° photograph. If the 0° scope showed any echoes, the antenna was raised to 15° elevation, and again the scope was photographed.
- c) If the 15° scope was clear, the data for the observation consisted only of the photograph of 0° and 15° . If the scope at 15° antenna elevation showed any echoes, the antenna was raised to 30° elevation angle, and again the scope was photographed.
- d) If the 30° scope showed any echoes, the antenna was raised to 45° elevation angle, and the scope was again photographed. If the 30° scope was clear, the data consisted of the three photographs 0° , 15° and 30° . If the scope was photographed at 45° , the data consisted of photographs from all four elevation angles.

Certain exceptions to the above rules had to be permitted to account for possible equipment failure and human resource limitations. If the staff at the station was preoccupied with other priority tasks, for instance,

monitoring of a storm, the observation could be missed entirely or the above sequence only partially completed. If the equipment malfunctioned, of course, there was no choice. The first type of exception has the potential of introducing bias in the sample because it could over represent fair weather conditions.

Information from the photographs was abstracted and recorded on coding sheets for each of the stations in the following fashion. For each photograph, an 80 column card image (line on the coding sheet) was to be prepared. The first fifteen columns were used to indicate/station/data/time/elevation angle/of the photograph. Column seventeen was to be left blank if there were any echoes on the photograph. Otherwise (if the photograph had no echoes) column seventeen would contain a "9".

Before the beginning of the experiment, two mutually perpendicular lines crossing at the center of the scope (the position of the radar antenna) were selected for each of the the stations. The selection was made on the basis of minimizing intersection with ground clutter at 0° elevation angle. The four rays generated by these two lines will be referred to as the "azimuth angles". Templates were made to be placed on each photograph. At 0° elevation each azimuth angle was marked off into 10 equal segments representing 10 nautical miles apiece. For each of the higher elevation angles the templates were marked off in seven equal subdivisions each one indicating an increase of 10,000 ft. in altitude at that elevation angle.

If no echo patterns intersected an azimuth angle, a "9" was place in the header column (see Table I-B-2) for that azimuth angle. Otherwise it was to be left blank. If a particular segment of one of the azimuth

angle was not intersected by echo pattern, the corresponding segment column of that azimuth angle was left blank (c.f. TABLE I-B-2).

Column sixty six was used to indicate that the scale was different from that used above. This occurred only one hundred forty times in the data from all seventeen stations. It was decided not to use such data but to leave them in the data base. Also, it should be mentioned that the inner ten mile radius was blocked out at elevation angle 0° since the intensity of the ground clutter image endangers the scope and makes reading of echo data from this region impossible.

The analysis of the radar photographs was made by meteorological technicians at the National Climatic Center (NCC) in Asheville, N.C. where the data were collated and punched directly onto two seven track magnetic computer tapes. Neither reel is magnetically labeled and both are written in buffered (long-stranger) record type. Each record is one hundred card images ordered by /station/year/month/day/hour/elevation angle/ in ascending order. The second tape consists of all 1974 and 1975 card images also with the above ordering. The first reel contains a total of 60,901 card images, the second 131,648. Thus the original tapes contained 192,549 card images.

Unexpectedly it was discovered that card images could not be equated with photographs. This is explained in the next subsection.

2. Culling the Radar Echo Data

The contents of the tapes were merged onto a single nine track magnetic tape and listed. The listing is over three thousand pages long. It was used to verify that all of the stations reported during every month of the study and that the data were in the advertised order. The listing also suggested a list of problems with card images which would have to be searched for and edited from the data.

The ordering of data was further checked using the CDC utility SORT/MERGE which operates on the "data key principal". At the same time, using SORT/MERGE, the data set was transferred to private disk pack STDATA. The new file incorporated all the information into the order scheme /station/year/month/day/hour/elevation angle/. It was discovered at this time that there were ninety card images from a mysterious station nineteen. This data was contained on the original tapes but was less noticeable when divided into small packets than when it appeared collected together in one place. Attempts to reclassify these data as belonging to other stations failed and they became the first data compiled on the list of card images to be sent back to NCC to be checked against the original coding sheets.

A first version of an editor program was written which scanned all 80 card image columns checking for impossible dates, station numbers, elevation angles, improper (non-numeric) characters, and information entered in improper columns. This program found several hundred more questionable card images for the list of problems to be sent to Asheville. It was learned that several stations would occasionally place the "9" indicating the scope was all clear in column nineteen (the header column for azimuth one) instead of column seventeen. If a "9" appeared in

column nineteen and the rest of the card image was blank, a "9" was added to column seventeen and column nineteen was made blank. If duplicates of a /station/time/elevation angle/ identifier were found, both cards were removed and added to the rectification list for NCC.

The list was sent to NCC for clarification. It contained approximately one thousand card images. In the meanwhile, a new editor was developed. It had several new features as well as all of the previous ones. It permitted merging data into the "buffer structure of the record" and it checked for a very peculiar problem. Card images had been accidentally discovered containing proper /station/time/elevation angle/ identifiers and nothing else recorded on them. Checking with the stations, the cause of this problem was found.

Stations would occasionally record the identifiers for observations in advance being certain that they would be made. Sometimes, such observations were not made or they were made but the photograph was not usable. The card image containing only the identifiers were not removed under the assumption that they would not be punched. But everything on the sheets was punched creating a number of "empty" observations. Surprisingly, the number of "empty" card images was nearly nine thousand; over eight thousand from one station alone. These would all have to be detected and deleted by the new editor.

Another task of the new editor was to enumerate the observation types for each station. An observation consists of one to four card images to be a "proper observation", according to rules (a) through (d), an observation begins with an elevation angle 0° card and ends with a card with "9" in column seventeen or with a card from elevation angle 45° .

Observation were classified using two hexadecimal digits. The first digit indicates which of the four card images are present. The second indicates which of the card images contains a "9" in column seventeen. The first digit would be "1" if only the card image for 0° is present, a "2" if only the card image for 15° is present, a "4" if only 30° is present and a "8" if only 45° is present. For further illustration, if 0° and 30° were present but not 15° and 45° , the first digit would be a "5" and if all four observations are present, the first digit would be hexadecimal "F" (or in decimal notation a "15"). The second digit characterizes the existence of clear scope indicators. An observation characterized as a "32" is an observation with 0° and 15° card images and a clear scope at 15° .

Certain observation types are clearly impossible, i.e., 14. Others are suspicious, i.e., 51. This is a case with two card images, one from 0° and one from 30° . The data from 0° indicates that the scope was clear. The card at 30° indicates that there is precipitation. A situation which is not impossible but not very likely. It would seem that what is likely in this case is that the 30° card had the wrong data punched on it. The only observation types consistent with (a) to (d) are 11, 32, 74, F8, or F0.

NCC eventually returned a report on the list of problems we had sent them. They had managed to unscramble over six hundred of them. Cards were repunched and verified at the Regis Research Center. The new editor had found new problems some of which Regis was able to unscramble. More data were punched and approximated, and eleven hundred new cards were re-inserted into the data base and were subsequently checked by the editor.

3. The Final Form of the Radar Echo Data Base

All card images surviving the culling described in § I-B-2 above are included in the current data base. It is written on both disc pack STDATA (permanent file GD5N) and on the nine track magnetic tape GD5M. In both cases it is buffered out as 100 card image records and required approximately 25000 PRU's of space. The tape is written at 1600 bits per inch and is magnetically labeled GD5M. Its records are of "long stranger" type on the CDC6600.

For actual use of the data base, a preselector of data was used. The preselector only processes card images of specified observation types. Two classes of observations were studied under the current Regis Contract; they are designated as Class A and Class B data. The set of Class A observations are characterized by the first type digit being a "1", "3", "7", or "F". Class B observations contain only observation types (1,1), (3,2), (7,4) and (F,8) and thus strictly adhere to the rules a), b), c) and d) stated in subsection I-B-1 of this report. For further clarification of the observation types and digits see TABLE I-B-3.

The amount of Class A and Class B data in the data base for each of the seventeen stations is enumerated in TABLE I-B-4.

<u>STATION</u>	<u>LOCATION</u>
1	ATLANTIC CITY, NJ
2	BRUNSWICK, ME
3	CHATHAM, MA
4	DAYTONA BEACH, FL
5	DETROIT, MI
6	HATTERAS, NC
7	HONDO, TX
8	JACKSON, MS
9	KEYWEST, FL
10	LIMON, CO
11	MEDFORD, OR
12	MIDLAND, TX
13	MINNEAPOLIS, MN
14	MISSOULA, MT
15	SACRAMENTO, CA
16	SAINT LOUIS, MO
17	SLIDELL, LA

TABLE I-B-1

The List of Stations Reporting Radar Echo Data Used in This Study

The data was originally gathered to produce a radar based climatology for a variety of locations with dissimilar climatological conditions. The data shows ground level and several other elevation angles which were concurrently measured by radar.

COL	USE
1-2	Station number (2 digits)
3	Always blank
4-5	Year (2 digits : 73, 74, 75)
6	Always blank
7-8	Month (2 digits : 1, ..., 12)
9-10	day (2 digits : 1, ..., 31)
11-12	Hour (2 digits)
13	Always blank
14-15	Elevation angle
16	Always blank
17	Observation header column (blank or 9) if "9" the scope is clear
18	Always blank
19	Azimuth angle 1 header (blank or 9) if "9" there are no echoes intersecting line
20-29	Azimuth angle 1 data
30	Always blank
31	Azimuth angle 2 header (blank or 9)
32-41	Azimuth angle 2 data
42	Always blank
43	Azimuth angle 3 header (blank or 9)
44-53	Azimuth angle 3 data
54	Always blank
55	Azimuth angle 4 header (blank or 9)
56-65	Azimuth angle 4 data
66	Special scale indicator

TABLE I-B-2

Card Format of Radar Echo Data

Azimuth angle data consists of the character blank representing zero or the digits one to eight. For elevation angle 0° all ten columns are used. For higher elevation angles only, the first seven columns are used.

<u>HEXIDECIMAL NOTATION</u>	<u>DECIMAL NOTATION</u>	<u>45°</u>	<u>30°</u>	<u>15°</u>	<u>0°</u>
0	0	N	N	N	N
1	1	N	N	N	Y
2	2	N	N	Y	N
3	3	N	N	Y	Y
4	4	N	Y	N	N
5	5	N	Y	N	Y
6	6	N	Y	Y	N
7	7	N	Y	Y	Y
8	8	Y	N	N	N
9	9	Y	N	N	Y
A	10	Y	N	Y	N
B	11	Y	N	Y	Y
C	12	Y	Y	N	N
D	13	Y	Y	N	Y
E	14	Y	Y	Y	N
F	15	Y	Y	Y	Y

TABLE I-B-3

The Two Digit Hexidecimal Classification System

The first digit is assigned a value from 0 - 15 according to the answers to the questions "does a record of the scope at elevation angle N exist in the data base?" for each value of N = 0°, 15°, 30° and 45°. In the above table "Y" represents *yes* and "N" represents *no*.

The second digit classifying an observation is assigned its value according to the question "was the scope recorded as being entirely clear at elevation angle N?".

STATION	NUMBER OF CARD IMAGES					# OF OBSERVATION	
	0°	15°	30°	45°	TOTAL	CLASS A	CLASS B
1	8123	2052	899	865	11939	8123	7427
2	8356	2723	851	550	12480	8356	7729
3	8330	714	353	121	9518	8330	6104
4	8121	3800	918	628	13467	8121	7177
5	7184	342	156	72	7754	7184	5475
6	7593	2888	508	253	11242	7593	6661
7	7683	893	142	73	8791	7683	6833
8	7677	1368	354	168	9567	7677	6302
9	6659	3055	736	410	10860	6659	4645
10	8326	919	238	74	9557	8326	7107
11	8173	1692	362	16	10243	8173	8052
	8101	1313	151	81	9646	8101	7632
12	7600	673	66	31	8370	7600	6852
13	7740	1409	244	84	9477	7740	7198
14	8507	459	98	17	9081	8507	7306
15	7611	2063	709	305	10688	7611	6878
17	8041	3399	1146	497	13083	8041	7205
TOTALS	133825	29762	7931	4245	175763	133825	116583

TABLE I-B-4

Itemization of Data Contained in Radar Echo Base

The above table itemizes both the number of cards and the number of observations for the two cases of observations described in this report (C.F. §I-B-3). The number of card images for a particular elevation angle is equivalent to the number of reports of information at that station and elevation angle for type A observation. The total number of cards is less than the total number for the entire data base which are neither type A or type B, e.g., an observation with data at 15° and 30° but none at 0°. This situation could arise if the 0° photograph was missing or unusable.

SECTION II

A GEOGRAPHIC COMPUTER DISPLAY SYSTEM



FIGURE II-A-1

Photograph of Globe and Projection

The viewer sees somewhat less than 180° of the sphere. The reference point chosen is Cairo (30°N , 30°E) and the point located is Sri Lanka (7°N , 78°E). The spherical triangle referred to in the text has the north pole and these two locations as its vertices. The Figure II-A-2 illustrates each of the coordinate systems referred to in the text.

The actual projection of latitude-longitude lines from this reference point is given later in Section II-B for several different radii between 30° and 180° . Unlike the above photograph both north and south pole is visible on some of the projections.

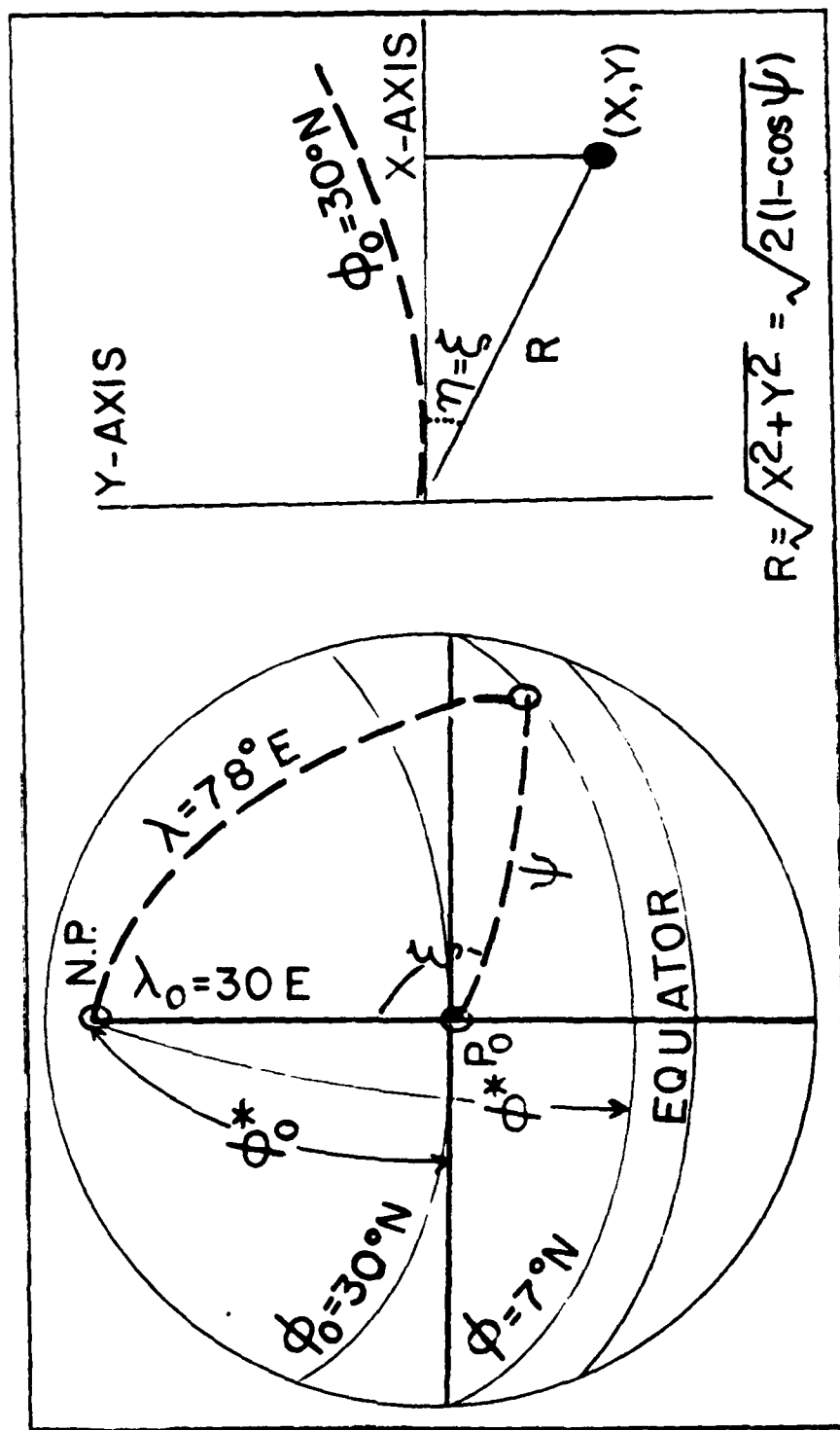


FIGURE II-A-2

Coordinate Systems of the Projection

On the left the (λ, ϕ) coordinate systems is shown as defined by point 30°N , 30°E (Cairo). The two heavy solid lines are great circles passing through Cairo. The one is the meridian line which projects to the y-axis on the right. The second is the great circle passing through Cairo tangent to $\phi = 30^\circ\text{N}$. It projects to the x-axis. ψ is the great circle distance from Cairo to Sri Lanka the point being located in this illustration (7°N , 78°E).

Notice that the x-axis is always south of $\phi_0 = 30^\circ\text{N}$ and eventually is as far south as $\phi = 30^\circ\text{S}$.

SECTION PREFACE

The computer display system described here permits automatic display of meteorological, climatological or statistical data referenced to the surface of the earth. The program is interactive. On cue, the user specifies the "types" of maps requested, the boundaries of the region and details of the background grid of longitude-latitude lines to be drawn, the maximum size of the map desired, and the file name on which the data is stored, (if it is to be automatically presented to the system). The option of plotting geographic, political and topological data, as well as data contours of physical quantities, are to be specified by the user.

The map is then displayed on the Tektronic scope and may be xeroxed and, if desired, sent to the facilities main CRT for hard copy photographs. A pen and ink capability is also optional.

SUBSECTION II-A

THE EQUATIONS OF TRANSFORMATION

The mapping procedure used was originally proposed by the Swiss mathematician, Johann Heinrich Lambert, in 1759 and is known as the Lambert azimuthal equal area map or sometimes simply as the equal area map. Its advantage over other more widely used projections is that on meso or synoptic scale it is relatively free of areal or angular distortion. On a global or greater than hemispheric scale it presents a comprehensible picture of large scale patterns.

Let $(\lambda, \phi)^1$ be the representation of the location of a point on the surface of the earth. The angle λ is its longitude, $\lambda = 0$ representing the Meridian at Greenwich, U.K.; λ increasing in the easterly direction ($-180^\circ \leq \lambda \leq 180^\circ$). The angle ϕ representing latitude ($-90^\circ \leq \phi \leq 90^\circ$), $\phi = 0$ representing the equator; ϕ increasing in the northerly direction. A point (λ_0, ϕ_0) will be specified and called the "reference point" of the projection. A second spherical coordinate system is specified in terms of the specified reference point. A point in the second coordinate system is given by the angular pair (ξ, ψ) .

An arbitrary point (λ, ϕ) in the first coordinate is expressed in the second (ξ, ψ) by equating ψ with the shortest great circle distance between (λ_0, ϕ_0) and (λ, ϕ) ; thus $0^\circ \leq \psi \leq 180^\circ$. The angle ξ between the meridian passing through (λ_0, ϕ_0) and the great circle arc connecting (λ_0, ϕ_0) to (λ, ϕ) by the shortest path measured in the clockwise direction. This is illustrated in Figures II-A-1 and II-A-2.

The point (λ_0, ϕ_0) corresponds to the degenerate circle $(\xi, 0)$ (actually the point $\psi = 0$), which is the "pole" of the second coordinate system. This new coordinate system is mapped onto a polar coordinate system on the plane (n, R) . It is in the specification of this transformation where Lambert's contribution is seen.

¹This section uses the coordinates in the order (λ, ϕ) rather than the usual climatological order of "latitude, longitude" because it is more suggestive of the (x, y) plot coordinates and because it is commonly used in papers in dynamic Meteorology.

The angle η is very simply expressed as:

1) $\eta = \xi$. (η is measured clockwise from the y-axis)

The radius R was given by Lambert as:

2) $R = (2(1-\cos\psi))^{\frac{1}{2}}$; $0 \leq R$,

The polar coordinate system (η, R) is then transformed into the Cartesian coordinate system which is fed into the plotting routines by the following elementary equations:

3) $X = R \sin \eta$ and

4) $Y = R \cos \eta$.

What remains is to convert an arbitrary (λ, ϕ) into (ξ, ψ) . From Figure II-A- it is apparent that triangle abc is a spherical triangle, and the law of cosines from spherical trigonometry may be applied to obtain:

5) $\cos\psi = \sin\phi \sin\phi_0 + \cos\phi \cos\phi_0 \cos\mu$; where $\mu = \lambda - \lambda_0$

and then the Pythagorean theorem yields:

6) $\sin^2\psi = 1 - \cos^2\psi$

completing the determination of ψ since $0 \leq \psi \leq 180$. ξ is also obtained through use of the law of sines and cosines:

7) $\sin\xi = \sin\mu \cos\phi / \sin\psi$ (again $\mu = \lambda - \lambda_0$) and finally,

8) $\cos\xi = (\sin\phi - \sin\phi_0 \cos\phi) / (\cos\phi_0 \sin\phi)$.

The area of the spherical disc with center (λ_0, ϕ_0) and of radius C is given by:

9) $A_c = \int_{-\pi/2}^{\pi/2} \int_0^C \sin\psi \, d\psi \, d\xi = 2\pi(1-\cos C)$

This spherical disc is mapped into a planar disc about the origin of radius $R = \sqrt{2(1-\cos C)}$ and of area A' :

$$10) \quad A' = \pi(2(1-\cos C)) = A_c.$$

Thus, the term "azimuthal equal area" is appropriate. The distortion to an arbitrary infinitesimal area element $d\psi d\xi$ on the sphere when it is mapped to the x-y plane is given by the following argument. Let β be any variable (for which $\frac{dR}{d\beta}$, $\frac{d\xi}{d\beta}$, and $\frac{d\psi}{d\beta}$ are defined at each point (ψ, ξ) on the sphere then:

$$11) \quad \frac{dR}{d\beta} = \frac{\partial R}{\partial \xi} \frac{d\xi}{d\beta} + \frac{\partial R}{\partial \psi} \frac{d\psi}{d\beta}.$$

Substituting ψ for β and using equation 5) this becomes

$$11a) \quad \frac{dR}{d\psi} = \frac{\partial R}{\partial \psi} = \frac{\sin \psi}{R} = \sin \psi (2(1-\cos \psi))^{\frac{1}{2}},$$

and thus the areal distortion of the mapping is shown in the following equation:

$$12) \quad dR d\eta = \frac{\sin \psi}{R} d\psi d\xi.$$

Distortion is seen to depend only on the distance of the region from the reference point. Table II-A-1 compares areal distortion with the value of the angular distance ψ . A map of a region of 15° radius or less has areal distortion of less than 1% and this distortion is mainly on the outer perimeter of the map.

The map is not conformal nor does it even preserve right angles. The analysis of angular distortion has been carried out and is very much more complicated to summarize than areal distortion. Its effects can be seen on the maps included in Figures II-B-1 and II-B-2.

ψ (in degrees)	Contraction
1	1.0000
5	0.9990
10	0.9962
15	0.9914
20	0.9848
30	0.9659
40	0.9396
50	0.9063
60	0.8660
70	0.8192
80	0.7660
90	0.7071
100	0.6427
110	0.5736
120	0.5000
130	0.4226
140	0.3420
150	0.2588
160	0.1736
170	0.0872
180	0.0000

TABLE II-A-1

Contraction of Infinitesimal Area Elements

The values listed are values of $\sin\psi/R$. The projected element is always smaller than element $d\psi d\xi$ but this is barely noticeable at synoptic scale. On a circle of radius 15° on the globe it is less than 1%.

Contraction refers to the ratio of the infinitesimal area element $dR d\eta$ on the x-y plane to the infinitesimal area element $d\psi d\xi$ at point (ψ, ξ) on the sphere.

SUBSECTION II-R

TWO TYPES OF REGIONS

The current computer program permits two types of regions to be mapped. The regions will be referred to as 1) "rectangular" and 2) "cameo". The boundary for a rectangular map is specified as rectangle in longitude-latitude coordinates. The map is always plotted with its geometric center in the center of the map plot but its reference point need not be the geometric center.

The boundary for the cameo method is a circle with center (λ_0, ϕ_0) , the reference point. The region is the locus of all points (λ, ϕ) whose great circle distance from (λ_0, ϕ_0) is less than or equal to an input radius ψ_0 . Cameo maps at present must always have (λ_0, ϕ_0) as their geometric center.

The application of the two types of regions are, 1) the rectangular region is convenient, esthetic and conventional for the meso and synoptic scales and permits labeling of longitude and latitude lines along the boundary; 2) the cameo was intended for large regions of hemispheric or greater scale and it does show large scale phenomena and its relation to a small included area to advantage (it is not without some appeal at small scale sizes).

Figures II-B-1 and Figure II-B-2 depict several examples of the Cameo type regions. They use Cairo (30°E, 30°N) as the reference point. Reference (9) presents several examples of the rectangular type region.

The map in Figure II-B-1 is made with $\psi_0 = 120^\circ$. This map corresponds to the photograph, Figure II-A-1. The photograph shows a plane intersecting

a globe at the distance of 120° from the point (30°E , 30°N). The map is a representation of everything on the sphere above the plane in the photograph. Notice that both the north and south poles are contained in the map but not the photograph.

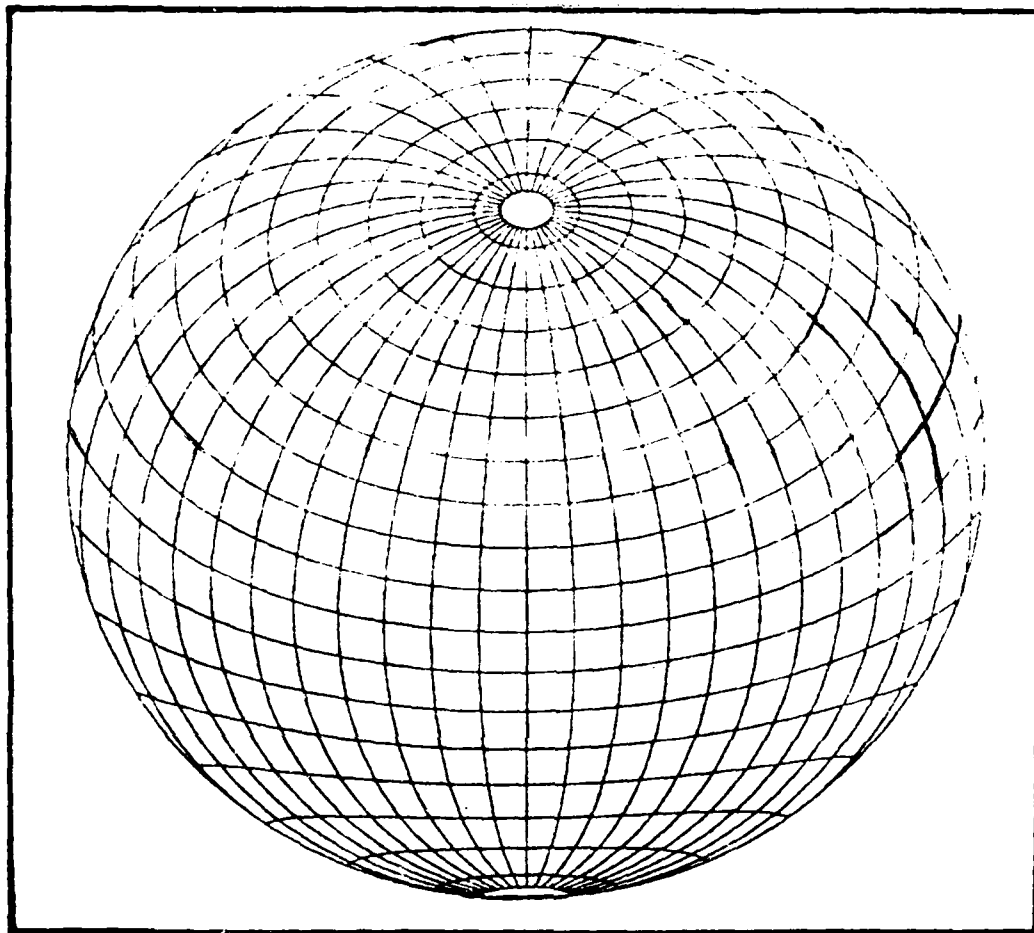


FIGURE II-B-1

Map of One Hundred and Twenty Degree Cameo Type Region

This displays, in Lambert equal area projection, the entire region of the globe above the plane intersection shown in the photograph Figure II-A-1. Notice that both the north and south polar regions appear in the above graphic. The map is centered at Cairo 30° E, 30° N and uses $\psi_0 = 120^\circ$. The latitude-longitude grid lines are spaced at 10°. The polar caps have 5° radius.

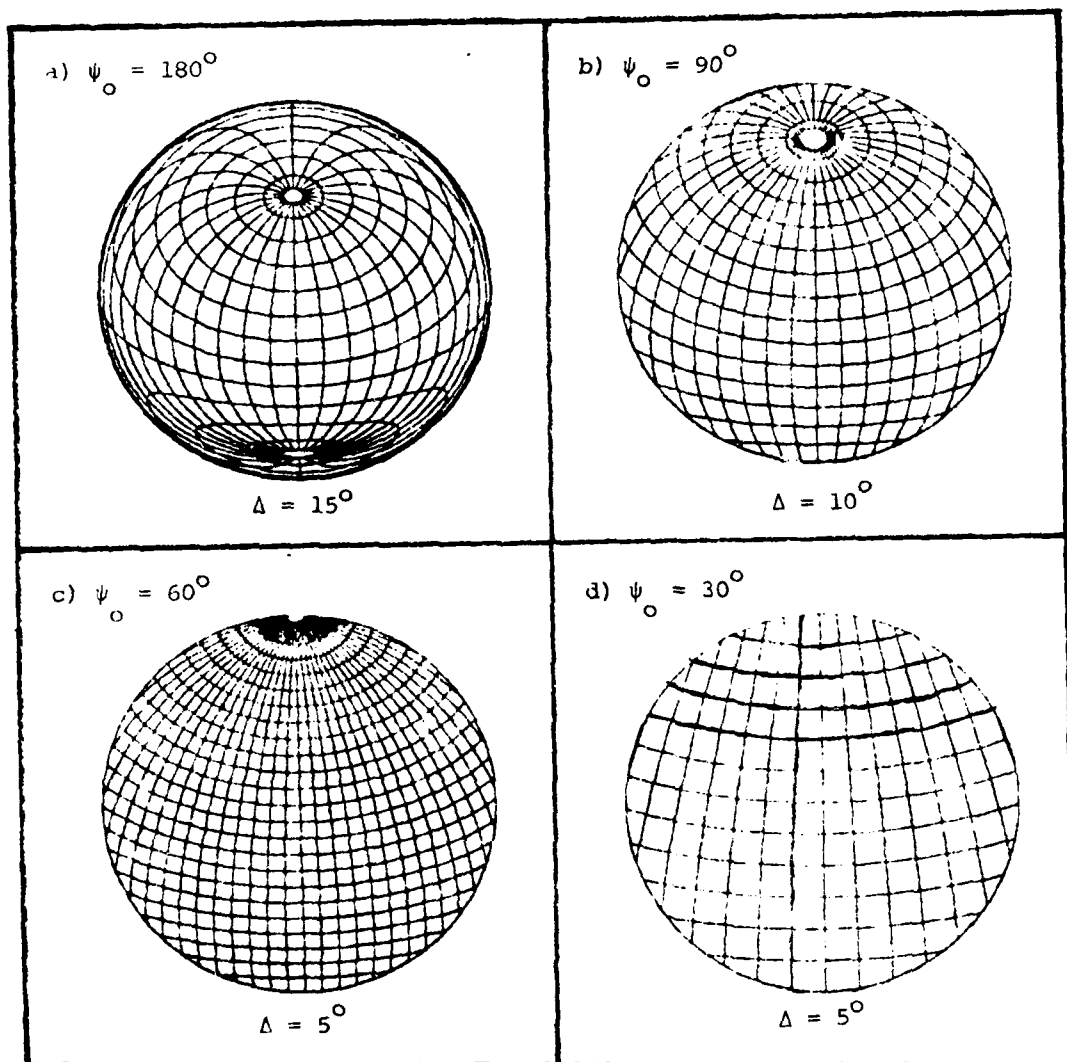


FIGURE II-B-2

Several Other Cameo Type Regions

All four of the above grids are drawn with the reference point $(30^\circ\text{E}, 30^\circ\text{N})$ as the geometric center. The spacing of latitude/longitude lines is indicated by Δ . The grid is aligned with the point $(0^\circ, 0^\circ)$. Notice that map a) shows both the north and south polar cap. The southernmost extent of d) is on the equator.

SUBSECTION II-C

DRAWING ARCS OF LATITUDE AND LONGITUDE CIRCLES: THE INTERSECTION PROBLEM

After the user defines, interactively, the region (type, locations and size) the system offers the option of specifying which longitude and latitude lines should be plotted on the map. The boundary of the region is always drawn on the map. It is possible to specify that the grid of latitude-longitude not be plotted. An example of the interactive question and answer process, used in the case of a cameo, is given in Figure II-E-1. This is a xerox copy from the Tektronic scope screen.

When a particular curve of constant longitude or latitude is chosen by the user, the program must find the points of intersections of the specified curve with the boundary of the region and draw only the portion of the curve which is interior to the boundary. This is a relatively simple task with the rectangular regions and a surprisingly intricate problem for the cameo type regions. The details of the method of solution of the constant longitude curve problems for cameo regions is given here. It is a paradigm for other intersection problems which arise in the drawing of geopolitical boundary and of contour data. The constant latitude curve problem is similar to the constant longitude curve problem but somewhat simpler.

Equation (5) can be used together with the Pythagorean theorem to obtain an equation for the sines and cosines of ϕ_i the values of latitude at which the intersection of the boundary and a given curve of constant longitude occur. A curve of constant longitude on the sphere is the arc

of a great circle passing from the south pole to the north pole. Let ψ_0 be the "radius" of the cameo with reference point (λ_0, ϕ_0) . Substitution into equation (5) gives:

$$13a) \cos \psi_0 = \sin \phi_1 \sin \phi_0 + \cos \phi_1 \cos \phi_0 \cos \mu$$

where $\mu = \lambda - \lambda_0$. Applying the Pythagorean theorem (3a) becomes:

$$13b) (\cos \psi_0 - (\cos \phi_0 \cos \mu) \cos \phi)^2 = \sin^2 \phi_0 - \sin^2 \phi_0 \cos^2 \phi$$

which is a quadratic equation in the variable $\cos \phi$. Using the classical quadratic formula two roots c_+ and c_- may be found which are possible values of $\cos \phi_1$:

$$13c) c_{\pm} = \frac{\cos \psi_0 \cos \phi_0 \cos \mu \pm \sin \phi_0 \sqrt{\sin^2 \phi_0 + \cos^2 \phi_0 \cos^2 \mu - \cos^2 \psi_0}}{\sin^2 \phi_0 + \cos^2 \phi_0 \cos^2 \mu}$$

and tentative values of the sines can be computed as:

$$13d) S_{\pm} = (\cos \psi_0 - c_{\pm} \cos \psi_0 \cos \mu) / \sin \phi_0.$$

If the quantity under the radical in (13c) is not positive, there are no intersection points. In this case the complete curve is either interior or exterior to the region. It is interior if and only if one point of the curve is interior. Two points are particularly easy to check and have special properties that make them of interest in themselves, they are the north pole and the south pole. The north pole is interior using (5) if and only if $\cos \psi_{N.P.} > \cos \psi_0$. But $\cos \psi_{N.P.} = \cos(\pi/2 - \phi_0) = \sin \phi_0$. Likewise the south pole is interior if and only if $\cos \psi_{S.P.} > \cos \psi_0$ and $\cos \psi_{S.P.} = -\sin \phi_0$ from which the relations:

$$14) \sin \phi_0 > \cos \psi_0 \text{ and}$$

$$15) -\sin\phi_0 > \cos\psi_0$$

become the criteria for the inclusion of the north pole and the south pole respectively in the interior of the region. If (14) is not satisfied, and it has been determined that there are no intersections, then nothing is plotted. If (14) is satisfied, the north pole is connected to the south pole with a curve of constant longitude.

If the radical in (13c) is positive, then C_+ and C_- are proper intersections if and only if $0 \leq C_{\pm} \leq 1$. If the value is greater than unity, it cannot be a cosine. If its value is less than zero, it could not be in the first or fourth quadrant and thus the latitude would not be between -90° and $+90^\circ$ i.e., the intersection is in another hemisphere. If neither C_+ nor C_- are proper intersections, the problem is treated as though the radical was negative.

If C_+ and C_- are both proper intersections, then if (14) is satisfied, (15) must also be satisfied. In this case, the north pole is connected to C_+ and C_- is connected to the south pole. If neither (14) nor (15) is satisfied, then C_+ is connected to C_- . If either C_+ is an intersection and C_- is not or vice versa, and if both (14) and (15) are satisfied, then the north pole is connected to the south pole (if this is the case, the curve must be tangent to the boundary at the proper intersection point). If only one of (14) or (15) are satisfied, then the existing proper intersection is connected to the interior pole. If both poles are exterior, an error has been made.

Latitude lines are not actually plotted all the way to the poles as too many lines converging on a point cause "blotting" in the case of pen

and ink drawing and "blooming" in case of CRT plots. The user is requested to supply a small radius about the poles. The system plots the projection of these small caps and terminates longitude lines on their boundaries rather than at the poles themselves. The same would be true of geopolitical maps and contours. Five degrees seems to work well on global scale maps and less may be used for smaller maps.

SUBSECTION II-D

CONTOURS AND GEOPOLITICAL BOUNDARIES

The term contour, in this section, refers to a collection of curves¹ on the surface of the sphere. Each of these curves will be referred to as a segment of the contour and a segment containing only one point will be called a degenerate. The system treats all contours uniformly, whether they represent geopolitical boundaries, topographical data, or curves of the constant values of a physical quantity. The line used to represent different contours may vary, i.e., the line width on CRT plots and the line types on pen and ink drawing or, whether and how lines are labeled, may vary according to the users specification but the basic format in which the data is presented is uniform. This section is concerned with the form of the basic data structure² employed by the system for contours.

The contour of a continental outline map with a rather skimpy resolution of 0.1° in longitude/latitude would require more than 50,000 points for the entire globe. Since each point is represented by two coordinates, in long form, this would take more than 100,000 words. This is an excessive amount of core for even the largest computer system and would be impossible at the AFGL computer center. The other extreme is to read the map into core one point at a time. This would require approximately one

¹Curve here means a geometric configuration homeomorphic with either a bounded closed interval of the real line or with a circle.

²A "data structure" in computer science is a data base containing implicit/explicit instructions on the location of the next piece of information and how it is to be processed.

minuted of I/O time for the simple example above. Considering the delays using intercom nearly ten minutes would pass before the map were drawn after the user requested it: painfully and impractically slow.

All practical mapping systems must follow a middle course between these two extremes. Unfortunately, the optimal course is machine dependent. The method described here uses two CDC 6600 special features, not common to other manufacturers' computing system. For this reason, care must be taken that the programming of contour input and processing be modular in nature and easily changed should AFGL change systems or if the program is to be used at other facilities.

The two special CDC features are the 60-bit word length and the BUFFER IN/OUT capability. The length, in bits, of each computer word determines the amount of information (longitude-latitude coordinator) and logic that can be packed into one word. The BUFFER IN feature allows the system to input one block of data simultaneously with the processing of a previous block. Since input time overlaps with the computation time, from the users standpoint, input time is of no practical importance using the BUFFER feature.³

A tentative format for the data structure for contouring in this system has been devised. Small auxilliary programs are needed to convert

³ At most modern computing facilities, AFGL included, I/O time is recorded separately from CPA time and is charged at a different and higher rate. Even so, the BUFFER feature is worthwhile because in an interactive environment it causes fewer and shorter delay time than conventional I/O methods.

existing computer map tables and the output of contour routines to accommodate this format and input record type.

Each segment begins with several "header" words. They include one word which contains the maximum and minimum values of λ and ϕ . If the segment does not intersect the region being mapped, the program skips immediately to the next segment. To accommodate this the header must also contain the relative location of the next segment in core.⁴ For convenience it also contains the length in number of points of the current segment.

A segment may cross the boundary of a specified map region any number of times which creates intersection problems that have some relationship to the intersection problem of the last section but are logically more complicated and their solutions will not be presented here.

Block or record length will normally be 512 words long. Thus, each block could contain up to 1024 points (four "numbers" are contained in each word and two "numbers" are required to describe each point on the globe). If a segment is not completed in a block, it continues at the first word of the following block. Each latitude is recorded as a 14 bit byte and each longitude as 15 bits. This permits a resolution of greater than one minute (actually to 1/64 of a degree) in both latitude and longitude.

The values are stored as binary integers. In latitude, for instance the south pole is represented by "0" and north pole as $2^{14}-1$ (in binary

⁴ If the current segment extends beyond the end of the current record being processed, the system detects this and waits until the next record is in core before processing can continue.

11111111111111). The integer is stripped from the word and converted to a floating point number which is then multiplied by $2\pi(2^{14}-1)$. The resultant floating point number is latitude (ϕ) expressed in radians ($-\pi/2 \leq \phi \leq \pi/2$). For longitude, a similar scheme is employed utilizing 15 bits instead of 14.

```

1 GO/ERASE
2 GO/SAVE
3 EXIT
ENTER OPTION:
TYPE OF GRID:
1.RECTANGLE
2.CAMEO
RESPONSE: 2
REFERENE POINT
DEC. DEG (LON/LAT): 30 30
12.RADIUS : 90
13.BOUNDARY
RESOLUTION: 100
14.INTERIOR
RESOLUTION: 125
15. SIZE: 4.3
16.X ORIGIN: 3
17.Y ORIGIN: 1
LONGITUDE LINES:
18.FIRST-180
19.LAST180
20.INCREAMENT10
LATITUDE LINES:
21.FIRST-90
22.LAST90
23.INCREAMENT10
24.POLAR CAP
(DEC. DEG.): 5
CHANGES?: 0

```

FIGURE II-E-1

Example of Interactive Query System

Computer-user dialogue xeroxed from the Kektronic scope. The first option is supplied by the system software. The user's response "1" after the word "option" indicates that all previous display is to be removed from the scope. Each of the subsequent questions 1 through 24 are asked by the Regis software. The answers supplied by the user in the above example define the graphic II-B-2 b) for $\psi_0 = 90^\circ$ (for more discussion see text II-E).

This dialogue appears in the right hand margin of the scope. The above figure is a 150% enlargement of the actual size produced on the xerox copy of the screen.

SUBSECTION II-E

THE CUEING SYSTEM: INTERACTIVE USE OF THE SOFTWARE

The primary method of creating a map using the system is through the textronic graphics terminal. The process is interactive, i.e., after certain preliminary instructions are supplied by the user, the program systematically requests information about the map and its construction from the user. Figure II-E-1 shows a xerox copy of the Tektronic scope during the initial input stage.

The program, in the of Figure II-E-1, first requests that the user indicate the type of boundary desired (this request for information is multiple choice). The user responds "2" - requesting a cameo boundary. The program then requests that the user supply the coordinates of the reference point; the user responds "30 30" (or 30° east, 30° north, the approximate coordinates of Cairo). This process continues until the program has enough information to draw the grid.

At this point, the program queries "CHANGES?". If the user, after examining the scope screen, decides that all answers he has given are as desired, he responds "0" and the program clears the screen and draws the grid - in the case of the example it is the grid in Figure II-B-2(b). If the user desires to change any of his previous responses, he responds with the number of the question. The program re-asks the question and the user supplies the correct answer. The program then responds again with "CHANGES?". The user has the option, at this time, to xerox the face of the Tektronic scope by pressing a button on the keyboard.

After the grid is drawn, the program enters a new phase. In the left hand margin it queries the user about contour overlays. After each contour has been specified, it is drawn on the map (either directly or as a separate overlay, as the user desires). The geopolitical boundaries themselves are a contour (C.F. Subsection II-D). As many contours may be drawn or overlayed to a map as is desired. When the user has finished with all of the contours, he indicates this to the program which then enters a third phase. Xeroxing may be done at any point that the user desires.

The third phase of the program allows the programmer to label the map and create a ledger. When this phase is completed, the user is given a choice of the disposition of the map, its overlays and labeling. The choices are simply to xerox them, send them to the computer center's CRT where slides will be produced, or to obtain pen and ink drawings of them. When sufficient information has been supplied to the program, this is done automatically and the program returns to the starting point again, ready for a new map.

It is also possible to run the program using cards, read in from the computer center or any of the high speed terminals. However, it is somewhat awkward to prepare the input for this type of operation.

SUBSECTION II-F

THE STATE OF COMPLETION

Not all features, discussed in this section, exist as completed software at the date of termination of this contract. A main framework of the program exists and is reliably running. Other parts are completed as "breadboard" construction and some are still in the experimental stage. Nearly everything mentioned in the preceding Subsections has been tried and found to work sufficiently well to be merged with the framework. The one major exception to this is labeling and ledgers. Although some experimentation has been done, the actual options to be included have never been finally decided upon.

The contouring features have been designed but the programming is still in the embryonic stage. This, of course, includes the drawing of geopolitical boundaries and topographical contours. A computer map of the globe, including political boundaries of North America, has been obtained and a portion of it has actually been plotted experimentally but the small program to convert it to the format, specified in Table II-D-1, has not been written. The map itself is of coarse resolution, particularly for mesoscale work. Work has been in progress improving the interactive cueing system and improving the grid system.

The plots, included in this report, required less than two seconds apiece to produce. It's expected that the computer maps or other contours will take approximately the same amount of time or less.

Certain ideas, not discussed previously in this report, have been investigated. They include the making of motion pictures displaying the development of global or large scale meteorological phenomenon and the drawing of three dimensional surfaces using the Lambert azimuthal equal area projection.

BIBLIOGRAPHY

References

- 1 Lund, I.A. and M.D. Shanklin, 1972 : Photogrammetrically determined cloud-free-lines-of-sight through the atmosphere. *J. Appl. Meteor.* 11, 773-782.
- 2 Lund, I.A., Gratham, D.D. Davis, R.E., 1980: Estimating probability of cloud-free-fields-of-view from the earth through the atmosphere. *J. Appl. Meteor.*, 19, 452-468.
- 3 Lund, I.A. and M.D. Shanklin, 1973 : Universal methods for estimating probabilities of cloud-free-lines-of-sight through the atmosphere. *J. Appl. Meteor.*, 12, 28, 35.
- 4 Plank, V.G., 1969 : The size distribution of cumulus clouds in representative Florida populations. *J. Appl. Meteor.*, 8, 46-67.
- 5 Pearson K., 1898: "Cloudiness: Note on a Novel Case of Frequency". *Proc. R. Soc. London*, 287-290.
- 6 Feller, W., 1967 *An Introduction to Probability Theory and Its Application*, 3rd Edition. John Wiley & Sons, New York.
- 7 Cramer, H., 1945 : *Mathematical Methods of Statistics*. Princeton.
- 8 Mandelbrot, B.N., 1977 : *Fractals : Form, Chance and Dimension*, W.H. Freeman & Company, San Francisco.
- 9 Gringorten, I.I., 1981. *Mapping the Climate*, AFGL-TR-81-0015, Meteorology division, Project 6670, Air Force Geophysical Laboratory, Hanscom AFB, MA.

Additional Bibliography

Scoree, R.S., 1972 : *Clouds of the World, A Complete Encyclopedia*, Stockpole Books, Harrisburg, Pa.

International Commission for the Study of Clouds (Deutsches Reich Reichsamt für Wetterdienst), 1939 : *Internationaler Atlas der Wolken und himelsansichten*, Berlin.

Ullman, J.D., 1980 : *Principles of Data Base System*, Computer Science Press, Potomac, Maryland.

END

DATE
FILMED

11-82

DTI